Specific detection of protein carbonylation sites by 473 nm photodissociation mass spectrometry

Romain Ladouce, Luke Macaleese, Karlo Wittine, Mladen Merćep, Marion Girod

Specific detection of protein carbonylation sites by 473 nm photo-dissociation mass spectrometry

Romain Ladouce[1,2], Luke MacAleese[3], Karlo Wittine[4,5], Mladen Mercep[1,2,4], Marion Girod[6]

[1] Zora Fundation, Ruđera Boškovića 21, 21000 Split, Croatia

[2] Mediterranean Institute for Life Sciences (MedILS), Meštrovićevo šetalište 45, 21000, Split, Croatia

[3] Univ Lyon, CNRS, Université Claude Bernard Lyon 1 – Institut Lumière Matière (iLM), LYON, France

[4] Department of Biotechnology, University of Rijeka, Radmile Matejčić 2, 51000, Rijeka, Croatia

[5] Selvita Ltd, Prilaz baruna Filipovića 29, 10000 Zagreb, Croatia.

[6] Univ Lyon, CNRS, Université Claude Bernard Lyon 1, Institut des Sciences Analytiques, UMR 5280, 5 rue de la Doua, F-69100 VILLEURBANNE, France.

Romain Ladouce ORCID: 0000-0003-2492-8180

Luke MacAleese ORCID: 0000-0001-8821-6049

Karlo Wittine ORCID: 0000-0002-0936-6709

Mladen Mercep ORCID: 0000-0003-1043-3486

Corresponding author: Marion Girod, Email: marion.girod@univ-lyon1.fr

ORCID: 0000-0003-0728-2111

Abstract

The study of protein oxidation remains a challenge despite the biomedical interest in reliable biomarkers of oxidative stress. This particularly true for carbonylations although, recently, liquid chromatography-mass spectrometry techniques (LC-MS) have been proposed to detect this non-enzymatic and poorly distributed oxidative modification of proteins using untargeted or carbonyl-reactive probe methods. These methods proved to be feasible but could not preserve the dynamic range of the protein sample, making it impossible to quantify oxidatively modified proteoforms compared with native proteoforms. Here, we propose an innovative method based on the implementation of a reactive carbonyl probe conjugated with a laser sensitive chromophore, dabcyl-aminooxy, which confers optical specificity to the LC-MS approach. In addition, our protein carbonyl detection method allows to localize individual carbonylation sites by observing fragments of derivatized oxidized peptides. Two model proteins, alpha-synuclein and beta-lactoglobulin, were oxidized and carbonylation sites were detected, resulting in the identification of respectively 34 and 77 different carbonylated amino acids. Thus, we demonstrated the application of a direct and sensitive method for studying protein carbonylation sites in complex protein extracts.

Keywords

chromophore derivatization, protein carbonylation, protein oxidative damage, laser induced dissociation, mass spectrometry.

INTRODUCTION

Proteins are the most abundant macromolecules in cells and therefore represent a major target for reactive oxygen species (ROS). Proteins are sensitive to oxidative stress and several oxidative modifications have been described [1]. Carbonylation is a non-enzymatic process with multiple causes (endo-/exogenous) and multiple effects on proteins [2]. Carbonyl groups, aldehydes and ketones, are the main biomarkers of oxidative stress [3, 4], and their concentration is low in the initial state and increases significantly during oxidative stress. Moreover, carbonyl groups are end products of the oxidation process, they cannot be removed and are stable. Therefore, protein carbonyl is a marker of redox status in biological systems and a biomarker of aging and age-related diseases [5–7]. The study of the whole protein carbonylation pattern, also known as carbonylome, can expand the understanding of the role of oxidative damage in protein homeostasis and cellular response. Carbonylation sites can likely be used as early biomarkers of oxidative stress-related diseases.

The detection and quantification of protein carbonylation have been extensively studied using hydrazide derivatives such as 2,4-dinitrophenylhydrazine followed by affinity-based detection methods: ELISA, 1D/2D Western blotting [8]. Hydrazones formed by the reaction of a carbonyl with a hydrazide are far less stable to hydrolysis than oxime bonds formed by the reaction of a carbonyl with an aminooxy [9]. In addition, the reaction yield of aminooxy-containing reagents with carbonyls is higher than that of hydrazide-containing reagents, making the use of aminooxy a suitable choice for bioconjugation methods [10–14].

Mass spectrometry (MS) is an important tool in modern proteomics. Bottom-up proteomics methods enable the identification of large numbers of proteins in complex mixtures based on the observation of unique peptides, reinforced by statistical approaches to validate protein identification. However, the observation of oxidative post-translational modifications (PTMs) in bottom-up proteomics is sporadic and entails low reproducibility of observations. Because oxidative modifications are non-enzymatic and non-specific, the number of potential modification combinations to take into account for each peptide becomes very important. Furthermore, the low abundance of oxidatively modified peptides makes the untargeted observation of oxidation sites by a bottom-up proteomics practically impossible unless an extensive enrichment of the subpopulation of oxidized proteins is performed with carbonyl reactive probes [5, 15–17]. This enrichment results in the

fractionation of the sample and reduces the possibility to obtain good quantification of carbonylated peptides compared to their non-oxidized forms.

Increased detection specificity toward a particular peptide subpopulation has been reported using laser-induced dissociation (LID) instead of the classical CID. Indeed, sulfonated peptides can be specifically detected by infrared multiphoton photodissociation (IRMPD) at 10.6 μm [18, 19]. In the ultraviolet range (UVPD), intrinsic chromophores such as disulfide bonds or tyrosine residues have also been used for specific detection [20, 21]. Grafting amino-acid side chains with appropriate chromophores is an alternative for introducing specificity at the fragmentation step. This concept was implemented using the judicious selection of chromophores absorbing in the UV at 351 nm [22] and 266 nm [23, 24] or in the visible range at 473 nm [25–27] for targeting Cys-containing peptides and pinpointing them in complex biological samples. We recently developed the visible LID-MS/MS coupling for streamlining the detection of Cys oxidized proteins thanks to proper derivatization of Cys-SOH with a chromophore tag functionalized with a cyclohexanedione group [28]. The elimination of the signal of interfering co-eluted compounds by LID-MS/MS enables the unbiased, sensitive and robust relative quantification of Cys oxidation within cohort samples.

Our current work presents a strategy coupling mass spectrometry and LID at 473 nm to increase the specificity towards carbonylated peptides in complex protein digests. A new dabcyl chromophore probe functionalized with an aminooxy group was designed in order to provide controlled grafting of carbonylated sites to confer a specific absorption property at 473 nm of oxidized peptides. To demonstrate the properties of the proposed method, we selected peptide and protein models. Leupeptin is a natural peptide with protease inhibitory properties that has the peculiarity of containing a carbonyl group. Therefore, it was a good opportunity to confirm the reactivity of Dabcyl-Aoo for the carbonyl group and to quantify the carbonyl derivatization reaction. Validation at the protein level was performed using α-synuclein and β-lactoglobulin protein models. Carbonylation site analysis for these two model proteins was performed under native and metal catalyzed oxidation (MCO) conditions, after trypsin digestion, without any enrichment step.

The current work demonstrates that the fragmentation specificity provided by LID results in the dramatic improvement in the signal attributed to carbonylated peptides in complex tryptic digests. This allows the detection and localization of multiple carbonyl residues. A targeted multiplex LID-Parallel Reaction Monitoring (PRM) strategy was therefore employed

to quantify the levels of derivatized carbonylated peptides from MCO proteins, and an oxidative ratio was calculated for each targeted peptide. The LID-MS/MS method implemented in this work opens doors to the characterization of preferential carbonylation sites and the determination of endogenous protein carbonylation levels for example in age-related disease cohorts.

MATERIALS AND METHODS

Chemicals and reagents

Boc-AoAc-NHS was purchased from IRIS Biotech (Germany) and dabcyl-C2-amine was purchased from Santa Cruz Biotechnology (USA). Silica gel 60 0.063-0.200 mm was purchased from Merck (Germany). Acetic acid, acetone, ammonium acetate, ammonium sulfate, streptomycin sulfate, trichloroacetic acid 20 % solution, tris(hydroxymethyl)aminomethane (Tris-Base) and urea were purchased from Serva. Ascorbic acid, ethylenediaminetetraacetic acid disodium salt dihydrate (EDTA), ethanol, hydrochloric acid (HCl) 37%, ferric (III) chloride ($FeCl_3$), leupeptin hemisulfate, sodium chloride (NaCl), dibasic sodium phosphate heptahydrate (Na_2HPO_4), monobasic sodium phosphate monohydrate (NaH_2PO_4) were purchased from Roth. The protein β-lactoglobulin A, DL-dithiothreitol (DTT), iodoacetamide (IAM), ammonium bicarbonate (AMBIC), and porcine pancreatic trypsin were purchased from Sigma-Aldrich.

Protease inhibitor mix was purchased from Cytiva. Human serum was purchased from Etablissement Français du Sang Pasteur (Lyon, France).

Optima® LC-MS Grade water (H_2O), methanol (MeOH) and acetonitrile (ACN) were obtained from Fisher Chemical and LC-MS Grade formic acid (F.A.) from Fluka. Solvents for NMR sample preparation were purchased from Eurisotop (Saint-Aubin, France). Anhydrous dimethyl sulfoxide (DMSO) for synthesis was purchased in a Sure Seal bottle from from Sigma-Aldrich (Saint Louis, MO, USA) and used via standard syringe technique. Solvents for column chromatography (dichloromethane DCM p.a and MeOH p.a.) were purchased from Fluka (Saint Louis, MO, USA), and Merck (Darmstadt, Germany) and were used without additional purifications.

Synthesis of dabcyl-ao-Boc

DABCYL-amine (100 mg, 0.32 mmol) and BocAoAsNHS (92 mg, 0.32 mmol) were dissolved in dry DMSO and stirred overnight at room temperature. The DMSO was removed by SpeedVac. The crude product was purified by column chromatography on silica gel 60 (Merck 0.063-0.200 mm), gravity chromatography was filled (packed) with SiO_2/ DCM and elution was performed with DCM/MeOH solution (40/1) to afford 86 mg of dabcyl-aminooxy-Boc (yield 55% orange-red solid).

Thin layer chromatography was performed on pre-coated Fluka 60A F254 plates and visualized with UV detection at 254 nm and 365 nm.

The structure of the synthesized compound was confirmed by NMR. ^{1}H NMR spectrum was recorded at 600.130 MHz for the ^{1}H nucleus using a Bruker AV600 spectrometer (Rheinstetten, Germany) at the NMR center of the Ruđer Bošković Institute in Zagreb (Croatia) (see Figure S1 in the Supporting Information). The sample was measured in deuterated chloroform ($CDCl_3$) at 25 °C in a 5 mm NMR tube with tetramethylsilane (TMS) as an internal standard.

Dabcyl-Aoo-Boc needs to be deprotected to obtain its carbonyl-reactive properties. Dabcyl-Aoo (DabAoo) was prepared by resuspension to 100 mM in an acetic acid solution containing 1 M HCl. The solution was incubated at 25 °C and 500 rpm for 1 hour. The solutions containing dabcyl should be protected from direct light to avoid decomposition. Solutions of DabAoo are stored at -18°C and stable for a month.

Alpha-synuclein expression in *E. coli* and purification

Protein expression and purification of α-synuclein was performed according to the publication by Volles *et al*. [29]. We obtained a culture of 200 mL with an OD_{600} of 0.7. From 100 mL of the *E. coli* culture, cell pellets were resuspended with 750 µL of lysis buffer (50 mM Tris pH8.0, 10 mM EDTA, 150 mM NaCl, 5 mM DTT, 1x protease inhibitor mix).

Samples were heated at 100°C for 10 minutes in a thermoblock followed by centrifugation at 15,000g for 5 minutes. To each 1 mL of supernatant, 136 µL of streptomycin sulfate and 228 µL of glacial acetic acid were added. After incubation at 4 °C for 30 min, the protein extract was centrifuged at 15,000 g for 5 min and the supernatant was collected.

A volume (1:1) of a saturated ammonium sulfate solution (saturated solution, 4 °C) was added to the protein extract, and the protein solution was incubated at 4 °C for 1 hour. The proteins were pelleted by centrifugation at 15 000 g for 2 min at 25 °C. The protein pellet was washed 2 times according to these steps: The proteins were resuspended in 900 µL of a 100 mM ammonium acetate solution. Then 900 µL of ethanol was added and the sample was incubated at 25 °C for 15 min. The protein suspension was centrifuged at 15 000 g for 2 min at 25 °C, and the supernatant was discarded. The protein pellet was then dried for a few minutes, then washed in cold acetone (-20 °C) and incubated at -20 °C for 15 minutes. The protein suspension was centrifuged at 15 000 g for 2 minutes. The pellet was dried for a few minutes.

Sample preparation

Leupeptin as a model of a carbonyl group-containing peptide.

Leupeptin was resuspended at 100 mM in water (H_2O). The derivatization reaction was performed with 1 mM leupeptin and 1.5 mM DabAoo and incubated overnight at 25°C and 500 rpm in the dark. The sample was dried using a SpeedVac and frozen.

For mass spectrometry analysis, the sample prepared with 1 µM in H_2O/MeOH (50/50) + 0.5% F.A. was directly infused at 3 µL/min.

In order to estimate the limit of quantification, the derivatized leupeptin was diluted in a complex digest of serum. For this purpose, 10 µL of human serum was mixed with 40 µL of 8 M urea and 5.5 µL of DTT at 150 mM in AMBIC 50 mM and then denatured at 60°C for 40 min. Samples were cooled to room temperature and 17 µL of 150 mM IAM in 50 mM AMBIC was added. Samples were stored in the dark at RT for 40 min and then diluted with 3 mL of 50 mM AMBIC. Digestion was performed with 10 µL of a 2 mg/mL trypsin solution at 37°C overnight. After digestion, samples were desalted and concentrated by SPE (Oasis HLB 3cc) and eluted with 1.5 mL MeOH [24]. The eluted samples were dried at 40°C in a N_2 stream and resuspended in 150 µL of a H_2O/ACN (90:10, v/v) +0.1 % F.A. solution, corresponding to the volume of spiked derivatized leupeptin.

Purified α-synuclein and β-lactoglobulin as a model.

A metal-catalyzed oxidation (MCO) reaction was used to generate carbonyl groups on the model proteins α-synuclein and β-lactoglobulin. A protein solution of 200 µg at 2 µg/µL in 10

mM phosphate buffer was oxidized by adding 25 mM ascorbic acid and 0.1 mM $FeCl_3$. The solution was incubated at 37°C and 500 rpm for 17 hours.

The MCO reagents were removed by protein precipitation as follows: 200 µg of the protein solution (100 µl) was placed in a microtube and 500 µL of cold (4°C) TCA 20% was added. The sample was incubated on ice for 15 minutes, homogenizing frequently. It was then centrifuged at 4°C for 5 minutes at 15 000 g and the supernatant was discarded. A volume of 1 mL acetone (-20°C) was added and the sample was incubated at -20°C for 1 hour, vortexing every 10 minutes. The sample was centrifuged at 4°C for 10 minutes at 15000 g, and the supernatant was discarded. The protein pellet was dried for a few minutes.

The protein was resuspended at 2 µg/µL in a solution containing 8 M urea and 30 mM phosphate buffer pH 7.0. Protein samples were labeled with 1 mM DabaAoo for 17 hours at 10°C with stirring at 500 rpm in the dark. The excess DabAoo was removed by protein precipitation as described above. The protein pellet was stored frozen.

For proteomic MS analysis, the derivatized MCO protein samples were denatured and reduced with 40 µL urea 8 M, 5.5 µL DTT 15 mM at 60°C for 40 min, and then alkylated with 35 mM IAM at room temperature in the dark for 40 min. In order to reduce urea concentration, samples were diluted 5-fold with AMBIC before overnight digestion at 37°C with trypsin using a 1:30 (w/w) enzyme to substrate ratio. Digestion was stopped by addition of formic acid at a final concentration of 0.5%. Samples were purified and concentrated by SPE as described above. All solutions were stored at -18°C before use.

Instrumentation and mass spectrometry operating conditions

Mass spectrometry analysis were performed on an hybrid quadrupole-orbitrap Q-Exactive® mass spectrometer (Thermo Fisher Scientific, San Jose, CA, USA) equipped with a HESI ion source coupled to a Surveyor HPLC-MS pump (Thermo Fisher Scientific, San Jose, CA, USA)[30] and a PAL Auto-sampler (CTC Analytics, Switzerland). This instrument has been modified to allow visible laser irradiation of ions by fitting a silica window on the rear of the HCD (Higher-energy Collisional Dissociation) cell. The laser is a 473 nm continuous wavelength laser (ACAL BFI, Evry, France). For LID analyses, the continuous laser is permanently turned on with an output power set at 450 mW. Ionization was achieved using electrospray in the positive ionization mode with an ion spray voltage of 4 kV. The sheath gas and the auxiliary gas (nitrogen) flow rates were respectively set at 35 and 10 (arbitrary

unit) with a HESI vaporizer temperature of 400°C. The ion transfer capillary temperature was 300°C with a sweep gas (nitrogen) flow rate at 5 (arbitrary unit). The S-lens RF was set at 90 (arbitrary unit). The Automatic Gain Control (AGC) target was 3e6 and the maximum injection time was set at 250 ms. Resolution @ *m/z* 200 in the orbitrap analyzer was set to 140,000 for the characterization of the chromophore and derivatized leupeptin.

The HPLC separation was carried out on a XBridge C18 column (100 X 2.1 mm, 3.5 µm) from Waters. The HPLC mobile phase consisted of H_2O containing F.A. 0.1 % (v/v) as eluent A, and ACN containing F.A. 0.1% (v/v) as eluent B. Elution was performed at a flow rate of 300 µL/min. The elution sequence, for the digested protein samples, included a linear gradient from 10 % to 60 % of eluent B for 52 min, then a plateau at 95 % of eluent B for 4 min. The gradient was returned to the initial conditions and held there for 4 min. The injection volume was 10 µL.

For the detection and identification of derivatized carbonylated peptides, experiments were performed in LID data-dependent top 10 mode. The full MS scans were recorded over a *m/z* 300-1500 range with a resolution of 35 000. For the data-dependent MS/MS scans, the resolution was set at 17 500 and the precursor selection was defined with a ±2 *m/z* window in order to select full isotopic patterns. A dynamic exclusion time of 20 s was set to exclude the redundant processing of dominant ions and allow selection of low abundant oxidized peptides.

Quantification was performed in PRM (Parallel Reaction Monitoring) mode with a resolution of 35 000 and a quadrupole isolation width of 2 Th. PRM lists of precursors are available in the Supporting Information Table S1.

For LID analysis, the activation time was set to 25 ms and the collision energy was set to 3 eV in order to allow efficient ion transmission but avoid higher-energy collisional dissociation (HCD) [26]. For HCD experiments, the activation time was set to 3 ms with an activation energy ranging from 19 to 24 eV depending on the precursor ion.

Identification and quantification of peptides

The fragmentation data was converted to peak lists using PAVA RawRead and searched against sequences of human α-synuclein (P37840) and bovine β-lactoglobulin (P02754) using Protein Prospector. The following parameters were used in all searches: mass tolerances in MS and MS/MS mode were 15 ppm and 0.02 dalton, respectively. Trypsin was designated as

the enzyme, with one missed cleavage allowed and a maximum of 2 modifications per peptide. Standard variable modifications were N-terminal acetylation and methionine oxidation. The maximum expected value allowed was set up to 0.01 (protein) and 1e-4 (peptide). For the search of oxidized peptides, user-defined variable modifications were implemented corresponding to a list of 11 known carbonyl modifications from the literature [31] derivatized with DabAoo. The affected amino acids and masses of the modifications with the DabAoo tag can be found in Table 1.

For quantification, performed in parallel reaction monitoring mode (PRM), using Skyline, the areas of 5 transitions corresponding to the 3 main peptide fragments and the 2 LID-specific fragments (*m/z* 252.11 and 148.09) were summed. The oxidation ratio was calculated by dividing the area of the derivatized carbonylated peptides by the area of the analogous non-carbonylated peptide quantified in top10-HCD (i.e., the sum of the precursor ion and the 3-4 specific fragment ions).

Table 1. List of oxidative modifications and affected amino acids as well as associated shifts in mass with the DabAoo tag

Acronym with DabAoo	Affected AA	Mass shift with DabAoo (Da)	Composition with DabAoo
Carb-1 DabAoo	R	323.126991	C(18), H(17), O(3), N(3)
Carb-2 DabAoo	M	334.171969	C(18), H(18), O(3), N(6), S(-1)
Carb-3 DabAoo	D,E	336.169859	C(18), H(20), O(1), N(6)
Carb-4 DabAoo	S,T	364.164774	C(19), H(20), O(2), N(6)
Carb-5 DabAoo	K	365.148790	C(19), H(19), O(3), N(5)
Carb-6 DabAoo	W	370.175339	C(18), H(22), O(3), N(6)
Carb-7 DabAoo	A,Q,E,I,L,W,Y,V	380.159689	C(19), H(20), O(3), N(6)
Carb-8 DabAoo	P	382.175339	C(19), H(22), O(3), N(6)
Carb-9 DabAoo	W, Y	398.170253	C(19), H(22), O(4), N(6)
Carb-10 DabAoo	W	414.165168	C(19), H(22), O(5), N(6)
Carb-11 DabAoo	W	430.160083	C(19), H(22), O(6), N(6)

RESULTS AND DISCUSSION

Characterization of the new chromophore DabAoo.

Recently, several aminooxy-based tandem mass tags were synthesized for covalent labeling of reactive carbonyls in proteins for affinity purification and immunoblot profiling [16]. Our strategy was to add a chromophore group to the aminooxy probe (Aoo) to generate absorbance properties in the visible range. The dabcyl chromophore is a non-fluorescent quencher used as an acceptor in Förster resonance energy transfer (FRET) applications. We have previously shown that grafting dabcylmaleimide results in high gas-phase photodissociation yields between 450 and 540 nm and is well suited for LID analysis [27]. Therefore, a new probe was designed that combines a reacting aminooxy group and a Dabcyl chromophore for specific derivatization of carbonyls moieties and for conferring to the final product absorption/photo-fragmentation property at 473 nm.

The protonated adduct of DabAoo-Boc is detected at *m/z* 485.2518 ($C_{24}H_{33}O_5N_6$, mass error: 1.236 ppm) in positive mode ESI-MS (Figure S2). The protonated dimer $[2DabAoo\text{-}Boc+H]^+$ is also detected at *m/z* 969.4963. The LID spectrum of the protonated DabAoo-Boc at 473 nm is shown in Figure 1a. Laser irradiation induces the depletion of the precursor ion signal and formation of several fragment ions.

The most intense ion at *m/z* 252.1112 is characteristic of the dabcyl chromophore and arise from the fragmentation between the carbonyl carbon and the ester oxygen. The LID fragmentation of the DabAoo-Boc chromophore also leads to the formation of two LID-specific fragments at *m/z* 120.0800 and *m/z* 148.0859 (see Scheme 1a). These reporter ions can be used to pinpoint derivatized carbonylated peptides from reconstructed ion chromatograms. The DabAoo-Boc chromophore has a high photo-fragmentation yield of 100 % after 3 ms of irradiation time.

Chromophore derivatization on the leupeptin model peptide.

The efficacy of DabAoo derivatization was investigated using leupeptin (N-acetyl-L-leucyl-L-leucyl-L-argininal), a natural tripeptide inhibitor of serine proteases containing a carbonyl group. The aminooxy group of the chromophore reacts with the carbonyl group of leupeptin by forming an extremely sT oxime bond after cleavage of the Boc group and a water molecule (the reaction is shown in Scheme 1b). The electrospray mass spectrum of the solution after the reaction shows a predominant doubly protonated leupeptin peptide $[M+DabAoo+2H]^{2+}$ at *m/z* 397.2493 ($C_{39}H_{62}O_6N_{12}$, mass error: 8.81 ppm), as well as a less intense singly protonated form at *m/z* 793.4856 (Figure S3). After elimination of the Boc

group, a residue of DabAoo is also observed at *m/z* 385.2001. Moreover, the derivatization reaction with DabAoo is quantitative, as only 1.5% of free leupeptin is detected. This reaction is specific and generates a stable product, oxime bond, so it can be used in a complex protein mixture. However, the presence of reagents containing primary amines may interfere with the aminooxy reaction toward carbonyls and may require the introduction of an excess of DabAoo.

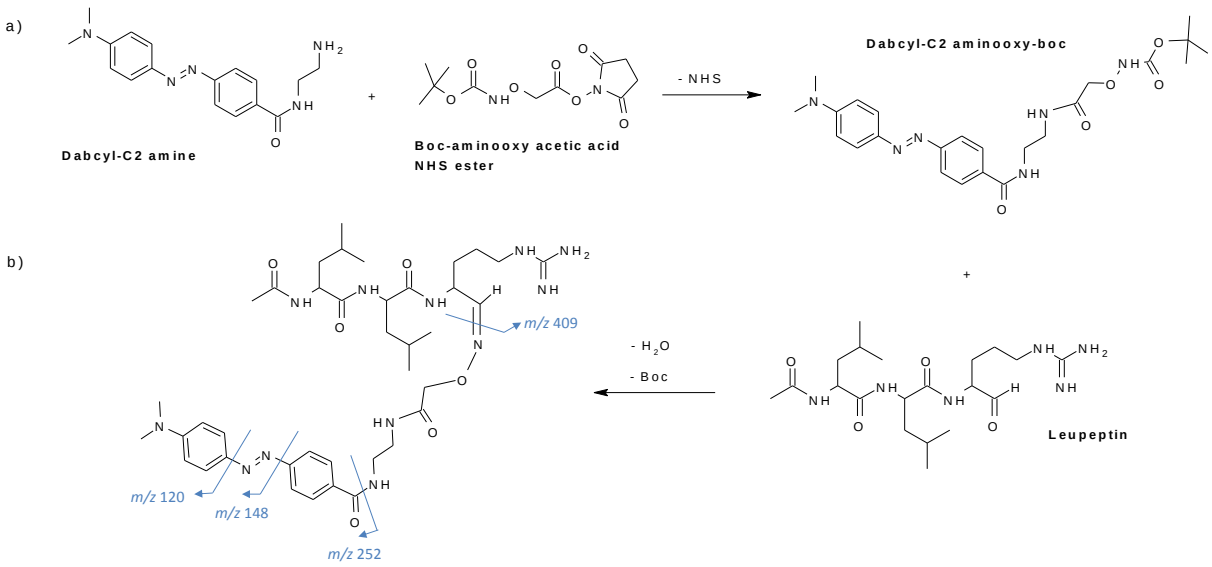

Scheme 1 (a) Synthesis of the Dabcyl-C2 aminooxy-Boc chromophore and (b) reaction with leupeptin

The LID spectrum of the doubly charged species at *m/z* 397.2495 (Figure 1b) exhibits intense reporter ions (*m/z* 252.1112, *m/z* 120.0800 and *m/z* 148.0857) arising from internal fragmentation within the chromophore that absorbs photons. In addition, b-peptide backbone fragmentations are detected throughout the system, which indicates some level of energy redistribution across the system and allows peptide sequencing. Fragmentation between the peptide and the chromophore linker is also observed from the precursor ion (*m/z* 409.2885 in Figure 1b and Scheme 1b). After 3 ms of irradiation, the photodissociation yield of the doubly charged derivatized peptide is about 98 %, a value only slightly lower than that of the DabAoo chromophore alone (100 % see Figure 1a). The high fragmentation yield achieved after a short irradiation time demonstrates the compatibility of the approach with chromatographic separation.

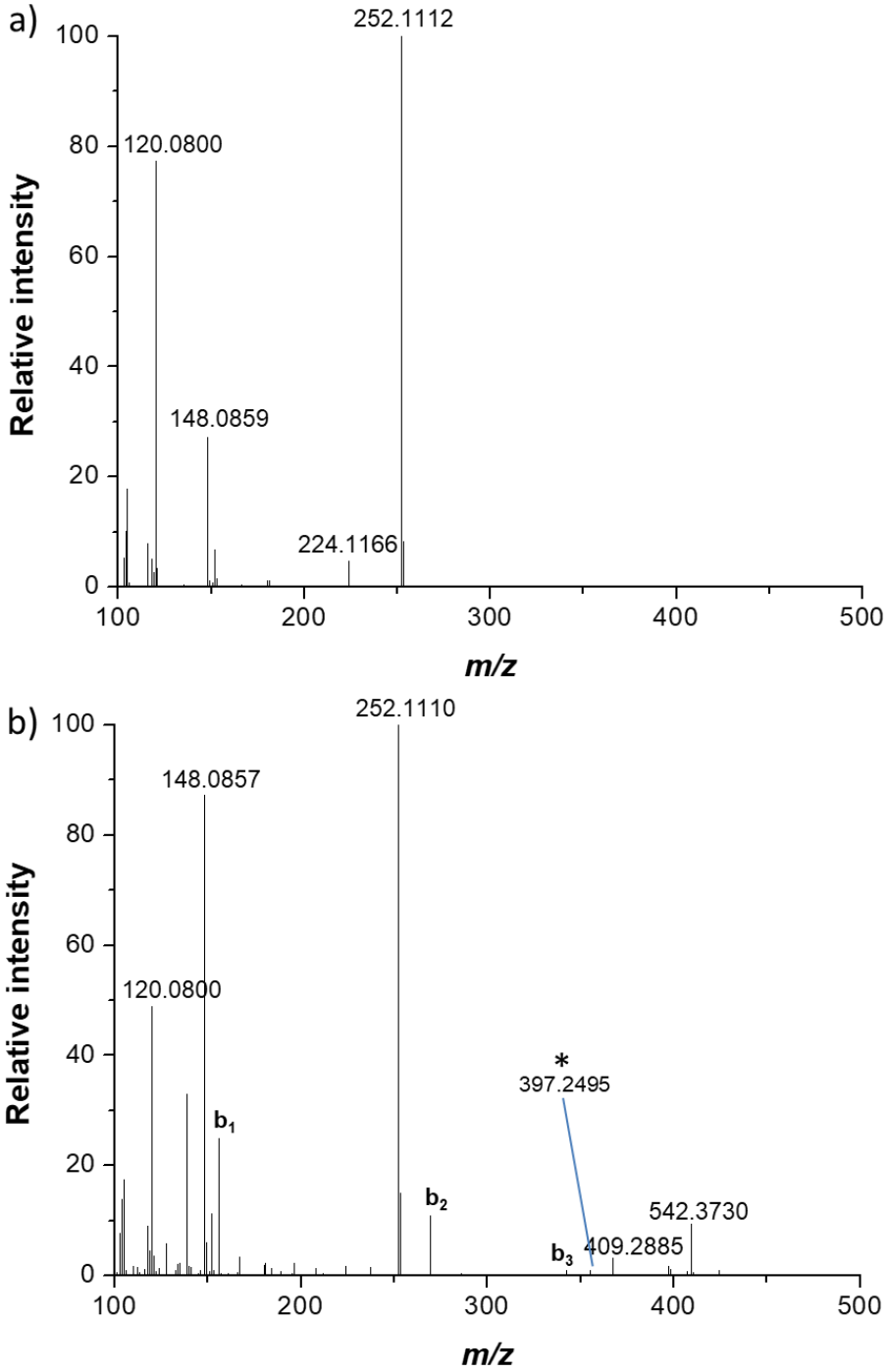

Figure 1 LID spectrum of a) the protonated DabAoo-Boc chromophore at *m/z* 485.2518 and b) the doubly protonated derivatized leupeptin $[M+DabAoo+2H]^{2+}$ at *m/z* 397.2495, both with 3 ms of irradiation time and laser power 450 mW. The asterisk shows the precursor ion. All ion assignments are supported by accurate mass measurements (errors <6 ppm). Fragment positions are shown in Scheme 1.

In order to evaluate the sensitivity and precision of the LID in top10 data dependent mode for the future detection of unknown carbonylated peptides, derivatized leupeptin was spiked into digested human serum to obtain final concentrations between 0.001 µg/mL and 3.3 µg/mL. Samples were analyzed by top10-LID, and semi quantification was carried out at the MS^2 level by summing the intensity of the precursor ion (*m/z* 397.24) and the 2 LID-specific fragments (*m/z* 252.11 and 148.08). The analysis of experiments performed in triplicate allows the determination of uncertainty windows: the coefficient of variation (CV) is below 20 % for all concentrations (Table S2). Figure 2a shows the XICs of the precursor ion *m/z* 397.24 in the full MS scans (black) and the 2 LID-specific fragments at *m/z* 252.11 and 148.08 (in blue and red, respectively) in the MS^2 scans for the lowest detectable concentration (i.e., 0.002 µg/mL leupeptin in plasma). At this estimated detection limit, the relative intensity of derivatized leupeptin at *m/z* 397.24 is only about 0.1% of the most abundant ion (see Figure 2b) but it is still selected for MS/MS in data-dependent mode (the corresponding LID spectrum at RT=29.72 min is shown in Figure S4).

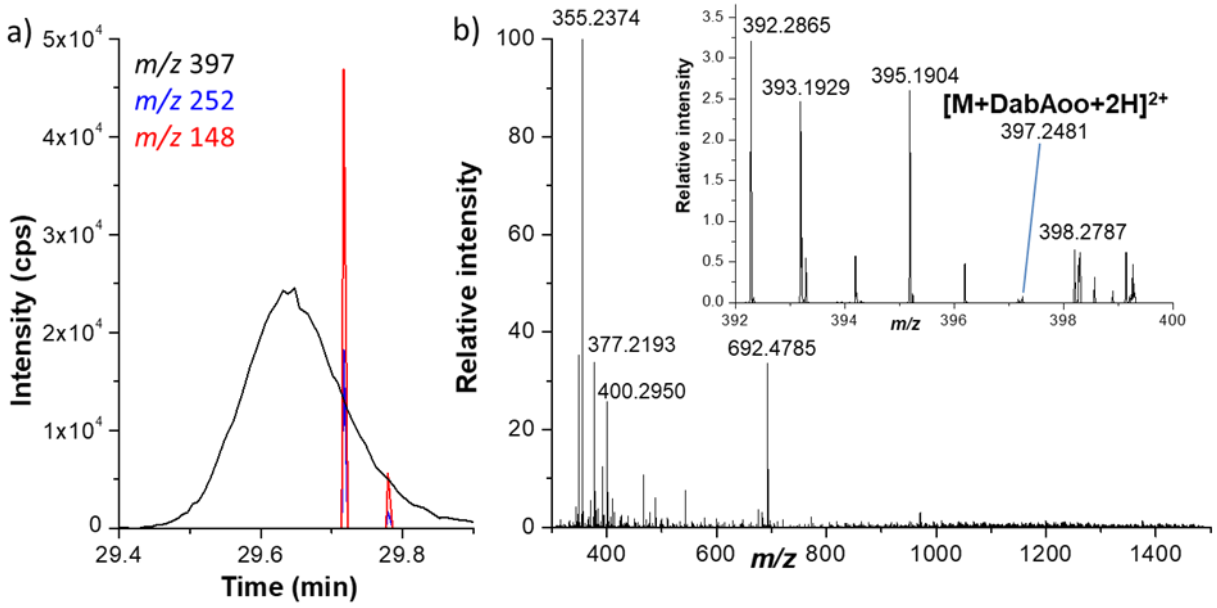

Figure 2 (a) Extracted ion chromatograms of the doubly protonated derivatized leupeptin at *m/z* 397.24 in the Full MS scans (black) and reporter ions *m/z* 252.11 (blue) and *m/z* 148.01 (red) in the MS2 scans, from the top10-LID analysis of the derivatized leupeptin at 0.002 µg/mL in plasma. (b) Corresponding averaged full MS spectrum between 29.6 and 29.7 min; the insert shows a zoom around the *m/z* of the doubly protonated derivatized leupeptin.

Specific detection of derivatized carbonylated peptides of MCO proteins

The applicability of the method to detect oxidized peptides in a complex proteome was evaluated for 2 model proteins: bovine beta-lactoglobulin and human alpha-synuclein (β-lacto and α-syn).

Parkinson's disease (PD) is a disease in which aggregation of α-syn forms inclusion bodies in the brain [32]. The phenomenon of aggregation has previously been associated with the oxidation status of α-syn [33, 34]. Therefore, the detection of carbonylation sites on α-syn could contribute to the understanding of changes in membrane interaction and protein aggregation process. Bovine β-lacto is an abundant whey protein in milk. The effects on its secondary structures, the α-helix and β-sheet, were studied under conditions of oxidative stress [35, 36].

The proteins were first oxidized with MCO and the carbonyl groups were derivatized with the DabAoo chromophore. Then samples were analyzed in top10-LID mode. Figure 3a shows the total ion chromatograms (TIC) recorded in top10-LID mode from the derivatized MCO-β-lacto sample, while the superimposed extracted ion chromatograms (XICs) of the chromophore reporter ions at *m/z* 252.11 (in black) and *m/z* 148.01 (in blue) are shown in Figure 3b.

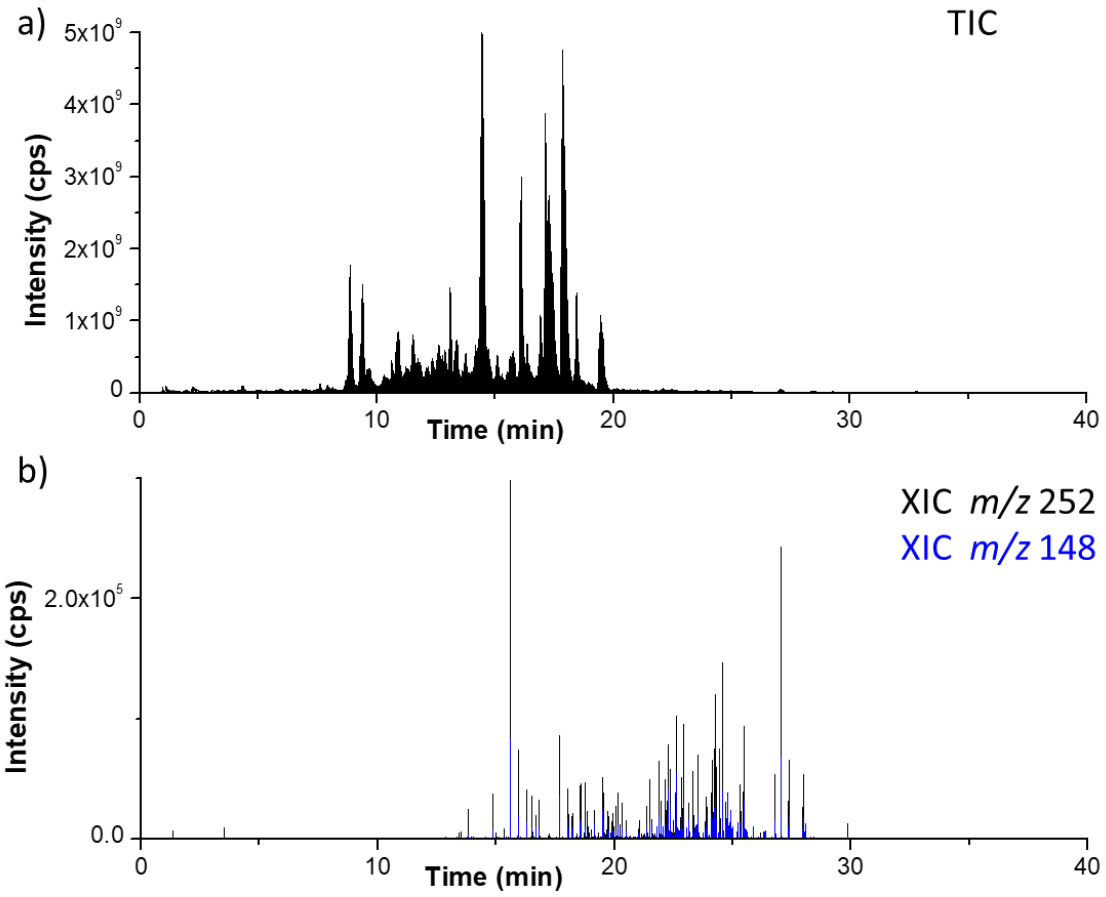

Figure 3 a) Total ion chromatogram of the top10-LID analysis of digested derivatized MCO β-lacto and (b) extracted ion chromatograms of the reporter ions *m/z* 252.11 (blue) and *m/z* 148.01 (black)

The same retention times are obtained for these two reporter ions, and comparison with the total ion chromatograms in Figure 3a shows that they are not observed for all peptides but only for specific derivatized carbonylated peptides. Thanks to the specificity of LID, only chromophore-derivatized compounds are fragmented, which allows accurate determination of carbonylated peptides in a complex protein digestion mixture. The same trend was observed for the derivatized MCO-α-syn sample (see Figure S5 in the supporting information).

The sequence databases were searched with of the LID-MS/MS data to identify carbonylated protein sites, i.e., modified peptides. The MS bottom-up proteomics approach is based on an algorithmic search of the peptide sequences. However, the search for multiple non-enzymatic PTMs leads to a combinatorial exponential increase in the search space and thus an increase in false PTM identifications. In the presented method, the DabAoo-grafted

peptide increases the delta mass of the PTM and enables the generation of a characteristic reporting ion. All MS/MS spectra of the identified derivatized carbonylated peptides were manually checked for confirmation and presence of the *m/z* 252.11 reporter ion (examples of MS/MS spectra can be found in Figure S6) as a proof of a DabAoo derivatized carbonylated site in the fragmented peptide. Since derivatized oxidized Arg and Lys residues are most likely not subjected to trypsin hydrolysis, one missed cleavage was included in the identification search against databases. In order to minimize the false positive rate, a maximum of 2 modifications per peptide was set. However, multiple derivatized carbonylated tryptic peptides will be in average larger and thus more difficult to ionize and detect. A combination of different enzymes could be envisaged to reduce their size, for instance Glu-C and trypsin. The list of peptides identified by Protein Prospector from the digested MCO-α-syn is shown in Table 2 (and Table S3 for the MCO-β-lacto digest sample). In total, 25 carbonylated DabAoo-modified peptides were identified with confidence in the derivatized MCO α-syn, corresponding to 34 different oxidized sites. Note that some non-derivatized peptides were also identified even with 3 eV HCD. For comparison, control non-oxidized samples were also derivatized with the DabAoo chromophore and analyzed by top10-LID. No derivatized carbonylated peptide was detected from control β-lacto digest sample (Table S3b) and only the AK[Car-5 DabAoo]EGVVAAAEK was identified in the α-syn digest control sample (Table S4).

Table 2: List of peptides identified in MCO derivatized with DabAoo MCO α-synuclein sample, using Protein Prospector from the top10-LID analysis. The bar between the AA numbers indicates different oxidized sites (i.e. precursor isomers) based on the mass of the fragment ions.

m/z	z	Peptide	Variable Mod @AA	RT (min)	Error ppm	Score	Expect
479.9201	3	AKEGVVAAAEK	Carb-5 DabAoo@2	17.35	-1.9	33.8	6.5e-9
358.2034	3	AKEGVVAAAEK		1.103	-3.8	16.9	8.9e-5
444.5618	3	EGVLYVGSK	Carb-7 DabAoo@4	18.83	-2.7	16.9	5.5e-5
515.9368	3	EGVLYVGSKTK	Carb-5 DabAoo@9	20.25	-6.5	27.1	7.7e-8
403.88	3	EGVVAAAEK	Carb-3 DabAoo@8	16.56	-10	21.1	2.9e-7
418.5437	3	EGVVAAAEK	Carb-7 DabAoo@1|3	15.85	-8.6	16	1.3e-5

418.5446	3	EGVVAAAEK	Carb-7 DabAoo@4	16.21	-6.4	19.1	2.3e-5
489.9204	3	EGVVAAAEKTK	Carb-5 DabAoo@9	17.08	-8.5	29.1	4.0e-9
734.3774	2	EGVVAAAEKTK	Carb-5 DabAoo@9|11	17.48	-7.9	19	2.5e-8
419.7166	4	EGVVHGVATVAEK	Carb-7 DabAoo@1|3	15.51	-6.3	21.4	7.0e-6
945.4897	2	EGVVHGVATVAEKTK	Carb-5 DabAoo@13|15	17.54	-7.7	21.4	3.5e-10
573.8082	4	EQVTNVGGAVVTGVTAVAQK	Carb-4 DabAoo@4	21.39	0.57	49.1	4.5e-11
577.8035	4	EQVTNVGGAVVTGVTAVAQK	Carb-7 DabAoo@14	18.92	-5.3	36.2	1.2e-12
573.8078	4	EQVTNVGGAVVTGVTAVAQK	Carb-4 DabAoo@15	20.55	-0.13	32.1	3.3e-9
764.7378	3	EQVTNVGGAVVTGVTAVAQK	Carb-4 DabAoo@12	20.08	-4.7	32.5	8.9e-11
577.8027	4	EQVTNVGGAVVTGVTAVAQK	Carb-7 DabAoo@1|2|3|6|9	20.38	-6.7	15.8	1.2e-8
770.0703	3	EQVTNVGGAVVTGVTAVAQK	Carb-7 DabAoo@6|9|10|11	18.83	-3.5	26.4	8.7e-9
414.6829	2	MDVFMK	Acetyl@N-term; Oxidation@5	10.82	-5.5	15	5.1e-10
374.1789	3	MDVFMK	Carb-2 DabAoo@1; Oxidation@5	19.72	-2.1	17.8	1.1e-6
512.9146	3	MDVFMKGLSK	Carb-5 DabAoo@6; Oxidation@1|5	23.16	-3	16.6	4.6e-5
1434.905	3	NEEGAPQEGILEDMPVDPDNEAYEMPSEEGYQDYEPEA	Oxidation@14	14.22	-6.6	21.5	8.6e-18
515.94	3	TKEGVLYVGSK	Carb-5 DabAoo@2	21.08	-0.28	25.9	3.8e-7
473.2508	4	TKEGVVHGVATVAEK	Carb-5 DabAoo@2	17.25	-3	30.6	2.6e-8
631.3404	4	TKEQVTNVGGAVVTGVTAVAQK	Carb-5 DabAoo@2	21.33	1.4	27.6	1.3e-9
475.5784	3	TKQGVAEAAGK	Carb-5 DabAoo@2	15.44	-5.1	18.8	5.2e-5
461.4924	4	TVEGAGSIAAATGFVK	Carb-4 DabAoo@1	21.52	-1.1	26.1	6.1e-9
614.9852	3	TVEGAGSIAAATGFVK	Carb-4 DabAoo@1|7	21.81	-4.8	19.1	1.0e-9
658.009	3	TVEGAGSIAAATGFVKK	Carb-5 DabAoo@16|17	22.30	-8.2	26.4	8.0e-11

To produce oxidized protein models, we have used *in vitro* oxidation (MCO). Therefore, the only type of protein oxidation will be direct oxidations of the amino acids side chains (see Table 1) while the formation of advanced lipoxidation and glycation end products (ALEs and AGEs) is not expected. For simplicity, carbonylations were annotated per chemical formula modifications. Hence, multiple amino acids can bear the same carbonylation type, see Carb-4, Carb-7 and Carb-9 in Table 1.

Amongst the 34 modified amino acids detected on derivatized oxidized α-syn, 14 are Carb-7 (-2H +1O, eight on V, three on E, one on Q, one on L and one on A), 13 are Carb-5 on K (-3H

+1O -1N), 5 are Carb-4 (-2H, four on T and one on S), 1 is Carb-2 on M (-1C, -4H, +1O, -1S) and 1 is Carb-3 on E (-2H -1O -1C).

We have identified 77 carbonylated amino acids on oxidized β-lacto, 37 of them are modified as Carb-7 (-2H +1O, ten on L, seven on A, seven on V, seven on E, four on I, one on W and one on Y), 14 are Carb-3 (-1C -2H -1O, eight on E, six on D), 9 are Carb-4 (-2H, five on T and four on S), 8 are Carb-5 on K (-3H, +1O -1N), 4 are Carb-8 on P (+1O), 2 are Carb-9 (+2O, one on W and one on Y), 1 is Carb-2 on M (-1C -4H +1O -1S), 1 is Carb-10 on W (+3O), 1 is Carb-11 on W (+4O). The same amino acid can be oxidized in different ways. Thus, seven residues E that were detected oxidized as Carb-7 were also observed as Carb-3. Similarly, residue W35 was observed alternatively with oxidation types Carb-7, Carb-10 and Carb-11. Moreover, a same carbonylatedAA is also detected in several peptide precursors (due to digestion miscleavages or isomers), which mainly supports its identification. Furthermore, the use of a mixture of proteases (for example, Trypsin and Glu-C) might enhance carbonylation site identification by generating distinct proteolytic peptides [37].

Mechanisms of oxidation and tools for their prediction have been proposed based on a simple model of protein oxidation [38, 39], while the protein oxidation processes are much more complex [40]. Nevertheless, some of the presented protein carbonylation mechanisms are interesting, such as the accessibility to solvents and the sensitivity of AA patterns to carbonylation. Moreover, the mechanism of carbonylation progression could occur when the local structure of the protein is affected by an initial carbonylation initiating the loss of structural homeostasis of the protein domain, leading to the exposure of other AA previously protected by protein folding. This oxidation cascade could significantly affect the structure and function of the protein. As an attempt to correlate the oxidation susceptibility with the secondary structure, the spatial distribution of carbonylation sites on the two model proteins was represented on 3D protein structures (Figure 4) using UCSF ChimeraX [41].

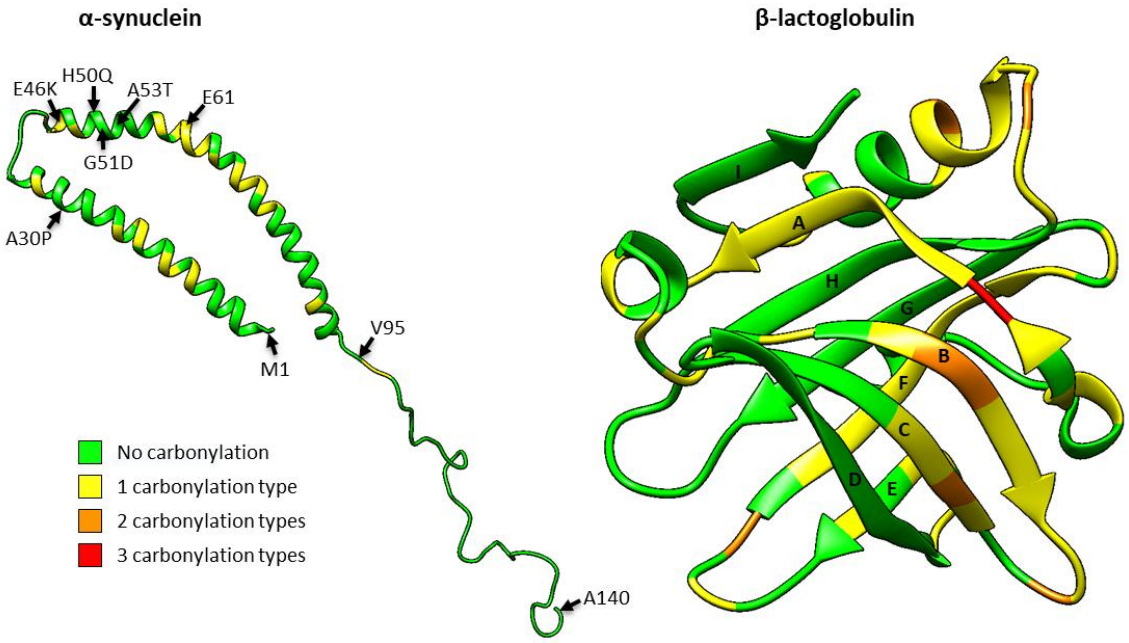

Figure 4 3D representation of the distribution of carbonylation sites on derivatized MCO α-syn (left) and β-lacto (right) from the top10-LID analysis. Amino acids colored in green do not present any modification and yellow, orange, red amino acids have been detected with respectively one, two and three different types of carbonyl modifications.

We can observe that the carbonylation sites on α-syn are close to the AA known to be mutated and responsible for familial Parkinson disease [42]. These mutations are A30P, E46K, H50Q, G51D and A53T while the nearest identified carbonylation sites are Carb-5 on K23, K34, K43 and K45, Carb-7 on E46 and V48 and again Carb-5 on K58. These oxidative modifications of the side chain of the AA could affect the protein structure since familial mutations are known to affect it. Overall, we detected 14 carbonylation sites in the N- terminal lipid- binding α- helix (AA 1-61), 13 in amyloid- binding central domain (AA 61-95) and 2 in C- terminal acidic tail (AA 95-140) (Figure 4 left panel).

β-lacto has been studied in detail in the context of milk processing and the effect of oxidation on protein structure were demonstrated in the publication by Du *et al.* [43]. In the latter publication, only two types of PTMs observed are carbonylation: Carb-6 and Carb-8, respectively affecting lysine (K) and proline (P) residues. Five carbonylation sites were confirmed in our study: P64, P66, K107, P142, K151, although the used oxidation method with hydrogen peroxide was different. We found that carbonylation sites are present on the α-helix and on β-strands A, B, C, E and F of the protein, which should have a significant

impact on β-lacto folding (Figure 4 right panel). These observations confirm the connection between protein oxidation phenomena and protein key structural elements necessary for the overall structure preservation; studying the nature of this link is beyond the scope of this paper.

Carbonylated peptides relative quantification

Having assessed the analytical performances of LID-MS/MS with DabAoo for the detection of carbonylation, a LID-PRM approach was implemented for the quantification of derivatized carbonylated peptides from MCO proteins in targeted PRM-LID mode. Thus, a multiplexed LID-PRM assay was designed to track, in digested MCO α-syn and β-lacto samples, the derivatized carbonylated peptides identified above in top10-LID analysis. The area of oxidized peptides elution peaks/reconstructed chromatograms have been normalized by the areas of the corresponding non-oxidized peptides (quantified by PRM-HCD) in order to calculate the oxidative ratio for each modified site. Indeed, since no enrichment of the carbonylated proteins was performed, the amount of oxidized vs. non-oxidized peptide can be estimated from the same sample. PRM list of both derivatized carbonylated and non-oxidized precursors (*m/z*, charge and range of retention time) is available in the Supporting Information Table S1 for the 2 proteins. Remarkably, derivatized oxidized peptides shown a retention time shift due to the increased hydrophobicity of the chromophore group. This behavior should also improve their detection in highly complex tryptic digest by extracting them from the abundant non-derivatized peptides. Moreover, due to the high proton affinity of the DabAoo, charge states observed for derivatized peptides are often higher than for their native form.

Examples of chromatographic overlay of transitions observed for derivatized carbonylated peptides, as well as the corresponding sequence, are presented Figure S7. Several conformational stereoisomers are observed in Figure S7a)-c). Interestingly, the (Carb-7 DabAoo) **I**P**AV**FKIDALNENK peptide can be oxidized at 3 different residues and shows 3 well separated RT peaks on the chromatogram in Figure S7d. Based on the LID spectra, the third peak at 24.7 min has been attributed to the **I**(carb-7 DabAoo)PAVFKIDALNENK form. However, the 2 other peptides with derivatized carbonyls at A and V could not be resolved due to the absence of characteristic small b ions containing the modification. The high signal to noise ratios allow confident relative quantification of oxidized and non-oxidized peptides.

Figure 5 shows the ratios of Area(ox)/Area(NOx) for the different modified peptides detected in MCO α-syn (all values can be found in Table S5).

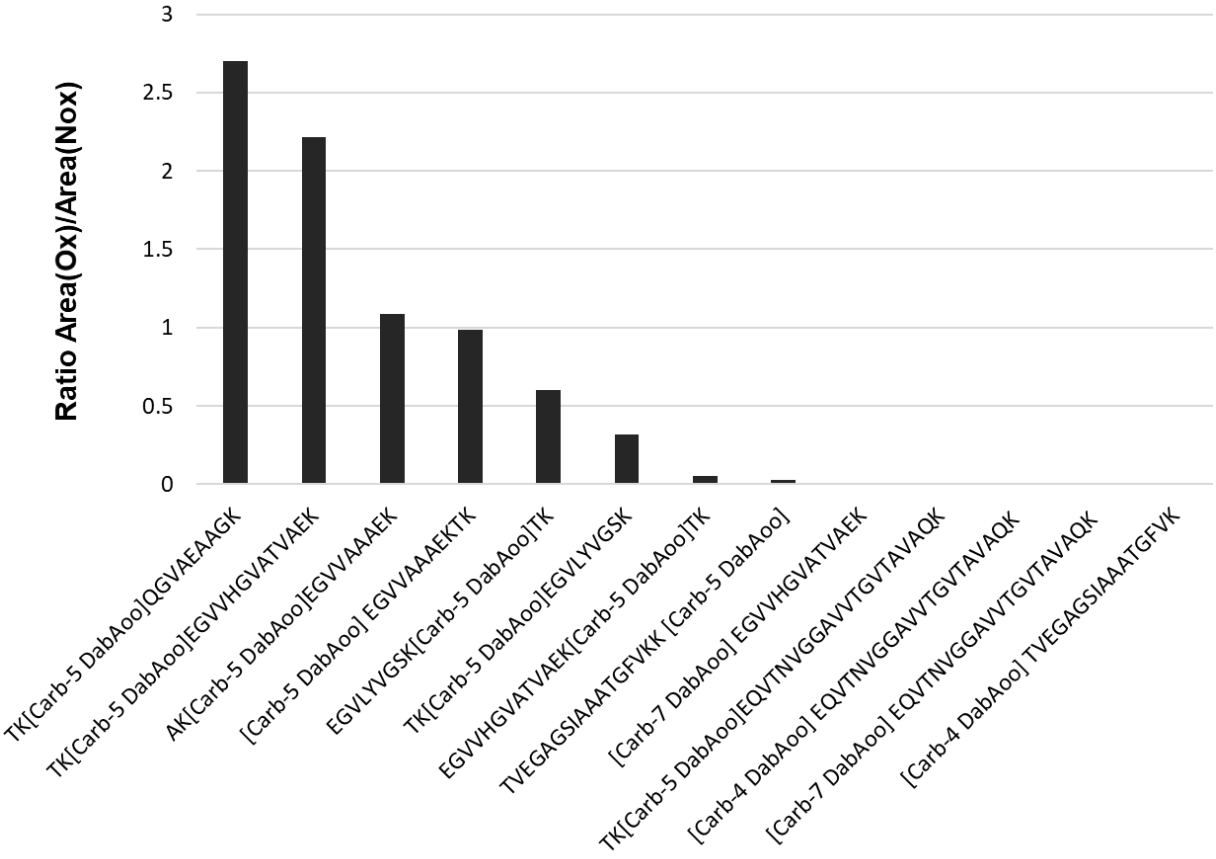

Figure 5 Oxidative ratio of each peptide for MCO α-synuclein sample: Peak area of the modified peptide, Area(Ox), divided by peak area of the corresponding non-modified peptide, Area(NOx)

Differences in oxidation levels can be observed between the different peptides. Two peptides present oxidative ratio above 2 (TK[Carb-5 DabAoo]QGVAEAAGK and TK[Carb-5 DabAoo]EGVVHGVATVAEK) with K23 and K34 as the most intense carbonylated sites. Similar signals of oxidized and non-oxidized peptides are observed for carbonylated AKEGVVAAAEK and EGVVAAAEKTK. Under the hypothesis that the response linearity is identical for the two forms, this corresponds to approximately 50% site occupancy. In any case, this high oxidative ratio confirms that Carb-5 on K is the major process. Oxidative ratio < 0.05 were obtained for the other quantified peptides indicating a low ratio of occupancy for these sites, and in general a low proportion of Carb-7 and Carb-4 on T and S processes.

For the MCO β-lacto (Figure 6 and Table S5), 4 peptides display oxidative ratio above 1 and 5 peptides show oxidative ratio between 0.2 and 0.6, while other oxidative ratio are < 0.05 . For this protein, Carb-7 and Carb-4 on T are the major observed processes and the most intense carbonylated sites are A96 and V97, followed by L103 and E105. Residues T113, V110 and L111 also present a high oxidation site occupancy.

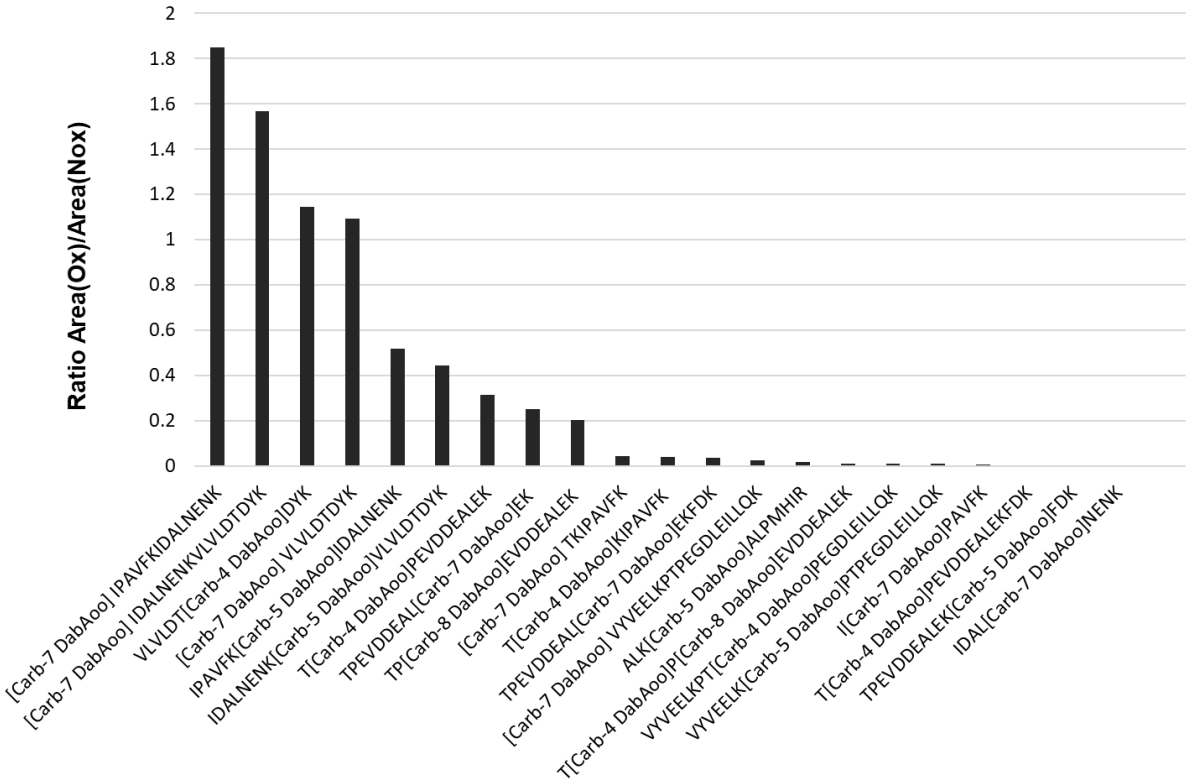

Figure 6 Oxidative ratio of each peptide for MCO β-lacto sample: Peak area of the modified peptide, Area(Ox), divided by peak area of the corresponding non-modified peptide, Area(NOx)

We can also note that the unique Carb-8 on P142 exhibit an oxidative ratio of 0.2 i.e. a non-negligible site occupancy.

This method enables the identification of carbonylation types and their quantification per site, which may provide an insight into oxidation pathways and mechanisms.

Conclusions

We have presented here a robust method for the detection of protein carbonylation sites in a complex mixture. Indeed, this method allows a direct and specific detection of the oxidized AA after grafting the chromophore by the reaction of the protein carbonyl group with the reactive aminooxy group. The derivatization reaction with the new dabcyl aminooxy chromophore (DabAoo) was first tested on carbonyl-containing leupeptin and then applied on *in vitro* MCO oxidized α-syn and β-lacto model proteins. Once grafted, derivatized carbonylated peptides are easily and specifically pinpointed during on-line 473 nm top10-LID analysis by reconstructing an ion chromatogram using a characteristic reporter ion at *m/z* 252.11. The LID fragmentation spectra of derivatized carbonylated peptides also exhibit intense y and b fragment ions arising from backbone fragmentation, which are essential for peptide identification in discovery shotgun proteomics. From the database search including 11 known carbonyl modifications, 34 carbonylation sites were identified from the top10-LID analysis of the MCO derivatized α-synuclein, including 28 detected in a single carbonylated peptide identification and 6 detected in two carbonylated peptides. Overall, 25 carbonylated peptides were observed for α-synuclein. We identified 77 carbonylation sites for the MCO derivatized β-lactoglobulin, 42 detected in a single carbonylated peptide, whereas 35 carbonylated sites were detected in more than one peptide. A total of 73 carbonylated peptides were detected for β-lacto. The developed method can confidently identify many carbonylated amino acids per proteins. This carbonylation sites should ideally be shared in a database such as CarbonylDB [44]. The robustness of this method is reinforced by the presence of the reporter ion at *m/z* 252.11 in the MS/MS spectra of the peptides as a proof a DabAoo grafted carbonylated site.

Even if in our experimental work oxidation on protein models was induced *in vitro*, we evaluate the localization of the detected carbonylation sites on the 3D structures of the proteins. We observed that most of the carbonylated sites are grouped and accessible for the solvent interaction. However, many structural parameters may influence the AA propensity to carbonylation, such as solvent accessibility, pKa or secondary structure. Moreover, protein carbonylation processes due to cellular oxidative stress may differ from our MCO models.

The method demonstrated good sensitivity with the leupeptin model, estimated at 0.003 µg/mL, using a top10 MS method. Moreover, targeted PRM-LID mode was used to quantify the main previously identified carbonylated peptides (13 for α-syn and 21 for β-lacto). Since

no enrichment of fractionation is required, we can compare the abundance of the carbonylated peptides and corresponding native forms in the same MCO sample. It is therefore possible to calculate an oxidative ratio for each peptide detected. This allowed to estimate the occupancy of the different carbonylated sites and the proportion of the total oxidized protein. Moreover, this normalization brings more accuracy for the comparison of carbonylation intensity within a group of cohort samples.

These results strengthen the concept that photo-fragmentation at 473 nm after chromophore tagging represents an effective strategy for specific detection and quantification of carbonylated peptides in large medical cohorts. Indeed, this method might be applied to investigate protein carbonylation in the human proteome, and possibly validate protein carbonylation sites as early biomarkers of human diseases.

Acknowledgments

The research leading to these results received funding from the French Agence National de la Recherche under the Grant Agreement ANR-18-CE29-0002-01 HyLOxi.

Molecular graphics performed with UCSF ChimeraX, developed by the Resource for Biocomputing, Visualization, and Informatics at the University of California, San Francisco, with support from National Institutes of Health R01-GM129325 and the Office of Cyber Infrastructure and Computational Biology, National Institute of Allergy and Infectious Diseases.

MG and LMA strongly acknowledge the invaluable support by Peter Baker at UCSF and Ruben Mascart at iLM for the local installation of ProteinProspector.

Supporting Information

^{1}H NMR spectrum of Dabcyl-amiooxy-Boc. Full MS spectra of the DabAoo chromophore and derivatization reaction of leupeptine with DabAoo. LID-MS/MS of three derivatized carbonylated peptides identified by ProteinProspector from the top10-LID analysis of MCO α-syn and β-lacto samples. Chromatographic overlay of transitions observed for derivatized carbonylated peptides. PRM precursors lists used for derivatized carbonylated and non-

carbonylated peptides screening in PRM. Precision and accuracy data on calibration samples for replicated derivatized leupeptin spiked at different concentration into human serum in top10-LID. List of peptides identified in MCO and control derivatized with DabAoo β-lactoglobulin sample, using Protein Prospector from the top10-LID analysis. List of peptides identified in control α-synuclein sample derivatized with DabAoo, using Protein Prospector from the top10-LID analysis. Oxidative ratio of detected carbonylated peptides quantified in MCO α-synuclein and β-lactoglobulin samples derivatized with DabAoo.

Accession Codes

Links to access the top10 results are provided in the Supplementary Material.

PRM-LID data are available via PeptideAtlas (http://www.peptideatlas.org/PASS/PASS05838).PASS01767).

Declarations

Conflict of interest The authors declare no financial or other competing interests.

References

1. Stadtman ER, Levine RL (2003) Free radical-mediated oxidation of free amino acids and amino acid residues in proteins. Amino Acids 25:207–218. https://doi.org/10.1007/s00726-003-0011-2

2. Fedorova M (2017) Diversity of Protein Carbonylation Pathways. Protein Carbonylation: Principles, Analysis, and Biological Implications 48–82. https://doi.org/10.1002/9781119374947.CH3
3. Dalle-Donne I, Rossi R, Giustarini D, Milzani A, Colombo R (2003) Protein carbonyl groups as biomarkers of oxidative stress. Clinica Chimica Acta 329:23–38. https://doi.org/10.1016/S0009-8981(03)00003-2
4. Girod M, Enjalbert Q, Brunet C, Antoine R, Lemoine J, Lukac I, Radman M, Krisko A, Dugourd P (2014) Structural Basis of Protein Oxidation Resistance: A Lysozyme Study. PLoS One 9:e101642. https://doi.org/10.1371/journal.pone.0101642
5. Fedorova M, Bollineni RC, Hoffmann R (2014) Protein carbonylation as a major hallmark of oxidative damage: Update of analytical strategies. Mass Spectrom Rev 33:79–97. https://doi.org/10.1002/mas.21381
6. Baraibar MA, Ladouce R, Friguet B (2013) Proteomic quantification and identification of carbonylated proteins upon oxidative stress and during cellular aging. J Proteomics 92:63–70. https://doi.org/10.1016/j.jprot.2013.05.008
7. Kehm R, Baldensperger T, Raupbach J, Höhn A (2021) Protein oxidation - Formation mechanisms, detection and relevance as biomarkers in human diseases. Redox Biol 42:101901. https://doi.org/10.1016/j.redox.2021.101901
8. Levine RL, Garland D, Oliver CN, Amici A, Climent I, Lenz A-G, Ahn B-W, Shaltiel S, Stadtman ER (1990) Determination of carbonyl content in oxidatively modified proteins. In: Methods in Enzymology. Elsevier, pp 464–478
9. Kalia J, Raines RT (2008) Hydrolytic stability of hydrazones and oximes. Angew Chem Int Ed Engl 47:7523–7526. https://doi.org/10.1002/anie.200802651
10. Ladouce R, Combes GF, Trajković K, Drmić Hofman I, Merćep M (2023) Oxime blot: A novel method for reliable and sensitive detection of carbonylated proteins in diverse biological systems. Redox Biol 63:. https://doi.org/10.1016/j.redox.2023.102743
11. Bollineni RC, Fedorova M, Hoffmann R (2013) Qualitative and quantitative evaluation of derivatization reagents for different types of protein-bound carbonyl groups. Analyst 138:5081–5088. https://doi.org/10.1039/C3AN00724C
12. Rojas Echeverri JC, Milkovska-Stamenova S, Hoffmann R (2021) A Workflow towards the Reproducible Identification and Quantitation of Protein Carbonylation Sites in Human Plasma. Antioxidants (Basel) 10:. https://doi.org/10.3390/antiox10030369

13. Afiuni-Zadeh S, Rogers JC, Snovida SI, Bomgarden RD, Griffin TJ (2016) AminoxyTMT: A novel multi-functional reagent for characterization of protein carbonylation. Biotechniques 60:186–196. https://doi.org/10.2144/000114402
14. Combes GF, Fakhouri H, Moulin C, Girod M, Bertorelle F, Basu S, Ladouce R, Bakulić MP, Maršić ŽS, Russier-Antoine I, Brevet PF, Dugourd P, Krisko A, Trajković K, Radman M, Bonačić-Koutecký V, Antoine R (2021) Functionalized Au15 nanoclusters as luminescent probes for protein carbonylation detection. Communications Chemistry 2021 4:1 4:1–11. https://doi.org/10.1038/s42004-021-00497-z
15. Bollineni RC, Hoffmann R, Fedorova M (2014) Proteome-wide profiling of carbonylated proteins and carbonylation sites in HeLa cells under mild oxidative stress conditions. Free Radic Biol Med 68:186–195. https://doi.org/10.1016/j.freeradbiomed.2013.11.030
16. Afiuni-Zadeh S, Rogers JC, Snovida SI, Bomgarden RD, Griffin TJ (2016) AminoxyTMT: A novel multi-functional reagent for characterization of protein carbonylation. Biotechniques 60:186–196. https://doi.org/10.2144/000114402
17. Lee S, Young NL, Whetstone PA, Cheal SM, Benner WH, Lebrilla CB, Meares CF (2006) Method to site-specifically identify and quantitate carbonyl end products of protein oxidation using Oxidation-dependent Element Coded Affinity Tags (O-ECAT) and nanoliquld chromatography fourier transform mass spectrometry. J Proteome Res 5:539–547. https://doi.org/10.1021/PR050299Q/ASSET/IMAGES/MEDIUM/PR050299QN00001.GIF
18. Borotto NB, McClory PJ, Martin BR, Hakansson K (2017) Targeted Annotation of S-Sulfonylated Peptides by Selective Infrared Multiphoton Dissociation Mass Spectrometry. Anal Chem 89:8304–8310. https://doi.org/10.1021/acs.analchem.7b01461
19. Wilson JJ, Brodbelt JS (2006) Infrared multiphoton dissociation for enhanced de novo sequence interpretation of N-terminal sulfonated peptides in a quadrupole ion trap. Anal Chem 78:6855–6862. https://doi.org/10.1021/ac060760d
20. Joly L, Antoine R, Broyer M, Dugourd P, Lemoine J (2007) Specific UV photodissociation of tyrosyl-containing peptides in multistage mass spectrometry. J Mass Spectrom 42:818–824. https://doi.org/10.1002/jms

21. Agarwal A, Diedrich JK, Julian RR (2011) Direct elucidation of disulfide bond partners using ultraviolet photodissociation mass spectrometry. Anal Chem 83:6455–6458. https://doi.org/10.1021/ac201650v
22. Cotham VC, Wine Y, Brodbelt JS (2013) Selective 351 nm photodissociation of cysteine-containing peptides for discrimination of antigen-binding regions of IgG fragments in bottom-Up liquid chromatography-tandem mass spectrometry workflows. Anal Chem 85:5577–5585. https://doi.org/10.1021/ac400851x
23. Diedrich JK, Julian RR (2011) Site selective fragmentation of peptides and proteins at quinone modified cysteine residues investigated by ESI-MS. Anal Chem 82:4006–4014. https://doi.org/10.1021/ac902786q.Site
24. Parker WR, Holden DD, Cotham VC, Xu H, Brodbelt JS (2016) Cysteine-Selective Peptide Identification: Selenium-Based Chromophore for Selective S-Se Bond Cleavage with 266 nm Ultraviolet Photodissociation. Anal Chem 88:7222–7229. https://doi.org/10.1021/acs.analchem.6b01465
25. Garcia L, Girod M, Rompais M, Dugourd P, Carapito C, Lemoine J (2018) Data-Independent Acquisition Coupled to Visible Laser-Induced Dissociation at 473 nm (DIA-LID) for Peptide-Centric Specific Analysis of Cysteine-Containing Peptide Subset. Anal Chem 90:3928–3935. https://doi.org/10.1021/acs.analchem.7b04821
26. Girod M, Biarc J, Enjalbert Q, Salvador A, Antoine R, Dugourd P, Lemoine J (2014) Implementing visible 473 nm photodissociation in a Q-Exactive mass spectrometer: towards specific detection of cysteine-containing peptides. Analyst 139:5523–5530. https://doi.org/10.1039/C4AN00956H
27. Enjalbert Q, Girod M, Simon R, Jeudy J, Chirot F, Salvador A, Antoine R, Dugourd P, Lemoine J (2013) Improved detection specificity for plasma proteins by targeting cysteine-containing peptides with photo-SRM. Anal Bioanal Chem 405:2321–2331. https://doi.org/10.1007/s00216-012-6603-5
28. Guillaubez J-V, Pitrat D, Bretonnière Y, Lemoine J, Girod M (2022) Relative quantification of sulfenic acids in plasma proteins using differential labelling and mass spectrometry coupled with 473 nm photo-dissociation analysis: A multiplexed approach applied to an Alzheimer's disease cohort. Talanta 250:123745. https://doi.org/10.1016/j.talanta.2022.123745

29. Volles MJ, Lansbury PT (2007) Relationships between the Sequence of α-Synuclein and its Membrane Affinity, Fibrillization Propensity, and Yeast Toxicity. J Mol Biol 366:1510–1522. https://doi.org/10.1016/j.jmb.2006.12.044
30. Guillaubez JV, Pitrat D, Bretonnière Y, Lemoine J, Girod M (2021) Unbiased Detection of Cysteine Sulfenic Acid by 473 nm Photodissociation Mass Spectrometry: Toward Facile in Vivo Oxidative Status of Plasma Proteins. Anal Chem 93:2907–2915. https://doi.org/10.1021/acs.analchem.0c04484
31. Rykær M, Svensson B, Davies MJ, Hägglund P (2017) Unrestricted Mass Spectrometric Data Analysis for Identification, Localization, and Quantification of Oxidative Protein Modifications. J Proteome Res 16:3978–3988. https://doi.org/10.1021/acs.jproteome.7b00330
32. Calabresi P, Mechelli A, Natale G, Volpicelli-Daley L, Di Lazzaro G, Ghiglieri V (2023) Alpha-synuclein in Parkinson's disease and other synucleinopathies: from overt neurodegeneration back to early synaptic dysfunction. Cell Death Dis 14:176. https://doi.org/10.1038/s41419-023-05672-9
33. Schildknecht S, Gerding HR, Karreman C, Drescher M, Lashuel HA, Outeiro TF, Di Monte DA, Leist M (2013) Oxidative and nitrative alpha-synuclein modifications and proteostatic stress: implications for disease mechanisms and interventions in synucleinopathies. J Neurochem 125:491–511. https://doi.org/10.1111/jnc.12226
34. Dias V, Junn E, Mouradian MM (2013) The Role of Oxidative Stress in Parkinson's Disease. J Parkinsons Dis 3:461–491. https://doi.org/10.3233/JPD-130230
35. Iwaoka M, Mitsuji T, Shinozaki R (2019) Oxidative folding pathways of bovine milk β-lactoglobulin with odd cysteine residues. FEBS Open Bio 9:1379–1391. https://doi.org/10.1002/2211-5463.12656
36. Krämer AC, Torreggiani A, Davies MJ (2017) Effect of Oxidation and Protein Unfolding on Cross-Linking of β-Lactoglobulin and α-Lactalbumin. J Agric Food Chem 65:10258–10269. https://doi.org/10.1021/acs.jafc.7b03839
37. Gu L, Robinson RAS (2015) Multiple Proteases to Localize Oxidation Sites. PLoS One 10:e0116606. https://doi.org/10.1371/journal.pone.0116606
38. Maisonneuve E, Ducret A, Khoueiry P, Lignon S, Longhi S, Talla E, Dukan S (2009) Rules Governing Selective Protein Carbonylation. PLoS One 4:e7269. https://doi.org/10.1371/journal.pone.0007269

39. Lv H, Han J, Liu J, Zheng J, Liu R, Zhong D (2014) CarSPred: A Computational Tool for Predicting Carbonylation Sites of Human Proteins. PLoS One 9:. https://doi.org/10.1371/journal.pone.0111478
40. Fedorova M (2017) Diversity of Protein Carbonylation Pathways. In: Protein Carbonylation. John Wiley & Sons, Ltd, pp 48–82
41. Pettersen EF, Goddard TD, Huang CC, Meng EC, Couch GS, Croll TI, Morris JH, Ferrin TE (2021) UCSF ChimeraX: Structure visualization for researchers, educators, and developers. Protein Sci 30:70–82. https://doi.org/10.1002/PRO.3943
42. Flagmeier P, Meisl G, Vendruscolo M, Knowles TPJ, Dobson CM, Buell AK, Galvagnion C (2016) Mutations associated with familial Parkinson's disease alter the initiation and amplification steps of α-synuclein aggregation. Proc Natl Acad Sci U S A 113:10328–33. https://doi.org/10.1073/pnas.1604645113
43. Du P, Tu Z, Wang H, Hu Y, Zhang J, Zhong B (2021) Investigation of the effect of oxidation on the structure of β-lactoglobulin by high resolution mass spectrometry. Food Chem 339:127939. https://doi.org/10.1016/j.foodchem.2020.127939
44. Rao RSP, Zhang N, Xu D, Møller IM (2018) CarbonylDB: a curated data-resource of protein carbonylation sites. Bioinformatics 34:2518–2520. https://doi.org/10.1093/bioinformatics/bty123

Graphical Abstract